Reliable and high quality adhesive bonding for microfluidic devices

Jingmin Li[1], *Chao Liang*[1], *Hao Zhang*[1], *Chong Liu*[1,2] ✉

[1]*Key Laboratory for Micro/Nano Technology and System of Liaoning Province, Dalian University of Technology, Dalian, 116024, People's Republic of China*
[2]*Key Laboratory for Precision and Non-traditional Machining Technology of Ministry of Education, Dalian University of Technology, Dalian, 116024, People's Republic of China*
✉ *E-mail: chongl@dlut.edu.cn*

Published in Micro & Nano Letters; Received on 15th August 2016; Revised on 12th October 2016; Accepted on 12th October 2016

Some issues, such as the removing of air bubbles from bonding interface, microchannel clogging by adhesive, the methods to increase bonding efficiency, as well as the adhesive bonding of a multilayer chip, still limit the use of adhesive bonding in the mass fabrication of microfluidic devices. In this work, an automatic adhesive bonding machine is developed which can obviously increase bonding efficiency and quality as compared with the traditional manually methods. A bonding method which uses a soft pressing head to extrude the air bubbles from bonding interface is presented. The relationship between the adhesive film thickness and the channel clogging is investigated. The adhesive bonding of three types of two-layer microfluidic devices and a five-layer microfluidic device are studied. Results have shown that the uses of the soft pressing head can effectively removing the air bubbles from the bonding interface. The bonding ratios of all devices are above 95%. The channel residual depth, which is the channel depth excluding the protrusion height of the adhesive film within the channel, will increase to follow the increase in microchannel width and adhesive film thickness.

1. Introduction: Bonding is an essential process in the fabrication of a thermoplastic microfluidic device [1–3]. Except the well-known methods, such as thermal bonding, microwave bonding, solvent bonding and ultrasonic welding [4–12], adhesive bonding, which includes liquid adhesive bonding and dry adhesive bonding, provides another alternative. Liquid adhesive bonding uses solvent or UV-curable adhesives to seal microfluidic devices. Im *et al*. [13] used a nano-scale adhesive layer to seal soft polymers or inorganic materials devices. Salvo *et al*. [14] employed SU-8 as glue to perform an adhesive bonding between two substrates with micro-patterned structures. Lutz *et al.* [15] used a thin layer of Epo-Tek 302-3M adhesive to achieve device bonding. In contrast, dry adhesive bonding uses dry adhesive, pressure sensitive film or adhesive tapes to achieve bonding. Farizah *et al*. [16] used a novel dual-cure dry adhesive to seal the microdevices at room temperature. Goh *et al*. investigated the bonding of polymer substrates by using PSA pressure sensitive film [17]. Tana *et al*. [18] used adhesive tapes to seal a polydimethylsiloxane-polymethyl methacrylate (PMMA) chip.

Several problems still limit the application of adhesive bonding in the fabrication of thermoplastic microfluidic devices. First, the removing of air bubbles from bonding interface and the avoiding of microstructures clog are still challenging [19]. Thermoplastic substrates are always inflexible to squeeze the air bubbles out of the bonding interface during bonding process. The trapped air bubbles may cause solution leakage as the microfluidic device is used for biological or chemical analysis. It also can lower the bonding strength. The bonding process can also cause the deformation of adhesive film or the flowing of liquid adhesive, which may result in the clogging of microstructures. However, there are still few studies on the air bubble and clogging issues. Second, most of the reported adhesives bonding methods have been done manually. It is time-consuming and difficult to guarantee the reproducibility of each microfluidic devices [20]. Moreover, a complete microfluidic device requires more than two layers to construct a 3D analysis system. To fabricate of a multilayer architecture microfluidic device by using adhesive bonding is difficult and has rarely been reported.

In this work, three kinds of two-layer microfluidic chips and a five-layer point-of-care testing (POCT) device were sealed by using pressure sensitive films. An adhesive bonding apparatus (ABA) has been developed to improve the bonding efficiency. A bonding method, which used a soft pressing head to remove the air bubbles from bonding interface and achieve bonding at room-temperature, is demonstrated. We call this method as SHP. The relationship between adhesive thickness, microchannel width and channel residual depth is investigated. The optimal adhesive bonding parameters are studied.

2. Fabrication

2.1. Development of an ABA: To enhance the bonding quality and efficiency, we developed an ABA (Fig. 1). It consists of the gas-liquid boost cylinder (GLBC), the pneumatic control system, the upper and under soft pressure head and the closed frame structure. The GLBC can provide higher and more stable pressure compared with the common-used cylinder. The working frequency of GLBC used in this apparatus is 30 min^{-1} and its working speed is 50–70 mm/s. It can provide the pressure up to 15 MPa. The pneumatic control system consists of a magnetic exchange valve, a speed control valve and a pressure regulating valve. These valves have the function of changing gas direction, controlling speed and pressure magnitude. The upper and under pressure head are made from silicon rubber, which can improve the quality of bonding and we will discuss it in the following parts. The effective working area of pressure head is 160 × 160 mm. This apparatus uses closed frame structure. Compared with open frame structure closed frame structure can enhance the structure rigidity and guarantee bonding quality.

2.2. Materials: In this work four different microfluidic chips (Fig. 1) are fabricated and bonded using adhesive bonding method. Among them, chip *a*, *b*, *c* are two layers, and their microchannel widths are different (Table 1). Chip d is composed of five layers. The channel structures are fabricated on a 50 μm-thickness adhesive tape. The other four layers are fabricated by using PMMA (AsahiKASEI, Japan). The substrates of chip *a*, *b*, *c* are fabricated by using hot-embossing (RYJ-1, DLUT, China), and every single layer of chip d is fabricated by CO_2 laser machining system (Fusion40, Epilog, UK). The 25, 50 and 100 μm thick adhesive tapes (ARclear Optically clear adhesive, Adhesive Research, Glen

doi: 10.1049/mnl.2016.0478

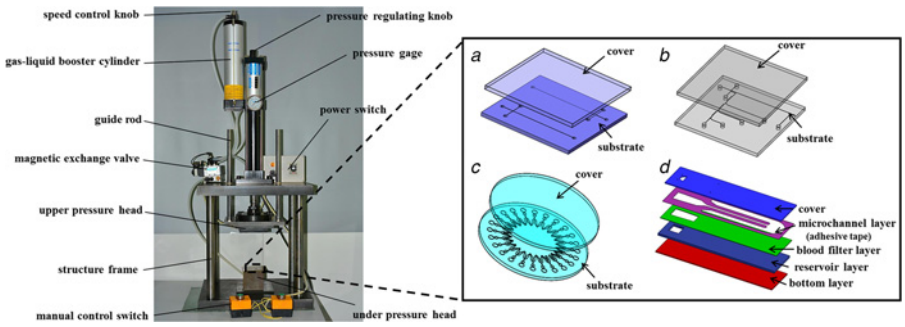

Fig. 1 *ABA and four bonded devices using this apparatus*

Table 1 Microchannel cross-section size (μm) for four kinds of chips

Types	Width	Depth
chip *a*	150	100
chip *b*	200	100
chip *c*	1000	100
chip *d*	2000	100

Rock, PA USA) used in this work are optical clear transfer films with long-term durabilities. The 180° peel adhesion of the film is 14.5 N/25 mm.

2.3. Substrate fabrication and bonding: Microstructures are replicated onto the substrates by using hot embossing with Si moulds. The adhesive tape is put onto the patterned substrate and the ABA is used to bond them together. The other side of the tape is peeled off. A cover plate is put onto the patterned substrate before using the ABA to bond. For five-layer chip *d*, first, adhesive tape is bonded with a PMMA substrate by using ABA. Then CO_2 laser is used to fabricate microstructures on the substrate. Second, the substrate is bonded with a blank substrate to form the base substrate of the chip. Third, the first process was repeated using different thick PMMA substrate to obtain different carrier layers. Finally, these carrier layers were bonded with the base substrate layer by layer. Besides that, multilayer chips which have more than five layers can also be fabricated using this bonding method (Fig. 2).

2.4. Bonding ratio (R_b) and channel residual depth (D_r) measurements: After the bonding process, in order to evaluate the bonding quality it is important to measure the bonding ratio and channel residual depth. The bonding ratio is the ratio of the sealed area (A_s) to the whole area of the chip (A_c) (Fig. 3*a*). The channel residual depth can be calculated by $D_r = D - T_a$, where D is the depth of the initial channel, T_a is the protrusion height of the adhesive film (see Fig. 3*b*).

The process of the bonding ratio measurement is as follows. A picture of the entire chip is taken first through a high pixel digital camera (Nikon D7100, Japan). To increase the contrast of the bonded area and the unbonded area, a white paperboard is put on chips. After picture processing, such as background removing,

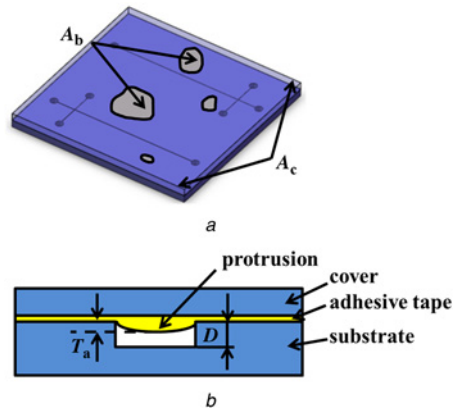

Fig. 3 *Schematic diagrams of bonding ratio and channel residual depth measurements*
a Bonding ratio R_b is A_s/A_c. A_s is the areas of the sealed area. A_b is the areas of the air bubble. A_c is the area of the entire chip. $A_s = A_c - A_b$
b Channel residual depth D_r is $D - T_a$. D and T_a are the depth of the initial channel and the protrusion height of the adhesive film, respectively

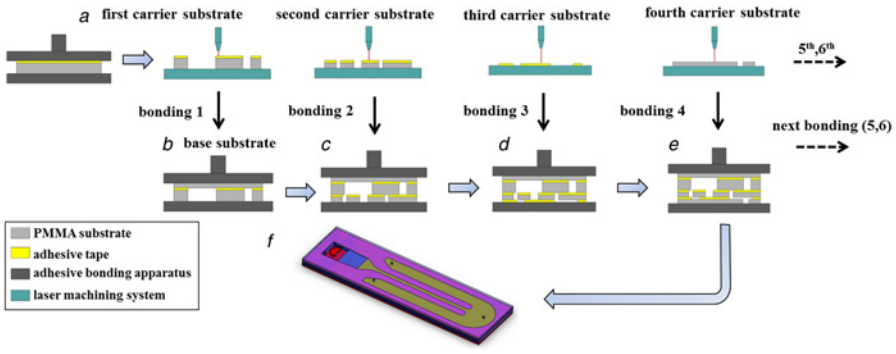

Fig. 2 *Adhesive bonding process for five-layer chip*
a Bonding adhesive tape with a blank substrate and laser machining the substrate, first carrier substrate
b Bonding the first carrier substrate with a blank substrate, base substrate
c–e Bonding the different thick substrate fabricated by laser machining system with base substrate
f Five-layer chip bonded

binarisation, median filtering, eroding and dilating, the ideal grey scales of the chips are obtained. Finally, white area A_c which represents the entire chip area and the black area A_b which represents the air bubble trapping area are calculated by using Matlab. Then the sealed area A_s is $A_c - A_b$. The bonding ratio can be derived as $R_b = A_s/A_c$.

To calculate the channel residual depth, the sample chips are cut off from the middle of the channels. After being frozen by liquid nitrogen, the pictures of their cross-sections are recorded with a measuring microscope (STM6, Olympus, Japan).

3. Results and discussions

3.1. Soft head pressing (SHP): To remove the bonding bubble from the bonding interface, a SHP method is performed. A 20 mm-thick silicon rubber (Wynca, China) is used as the material of the soft head. It is fixed onto the upper pressing head of the machine. In order to exhibit the different effects between SHP method and conventional hard pressure head (HPH) bonding on the bonding ratio, we choose four types of chips (*a*, *b*, *c*, *d*) to do the comparing experiments. The experiment for each type of chip is repeated 5 times. After experiments, we calculated the bonding ratios for SHP and HPH, respectively. Fig. 4*a* shows the bonding ratios obtained by using same process parameters. The results show that, by using SHP, the bonding ratio increases 20 to 43% for two layer chips (chip *a*, *b*, *c*) as compared with conventional HPH method. For the multilayer chip (chip *d*), the conventional HPH method only can achieve a bonding ratio below 20%. However, the multilayer bonding ratio by using SHP has reached 95%. It can be found that the SHP method is very effective in improving adhesive bonding ratio, especially for the multilayer devices. The entire process of bonding has been performed at room temperature, and the time-consuming for whole process is less than 1 min. The bonding process does not need clean laboratory environment. Moreover, after bonding process, the bonded chip has not thermal stress. The bonding strength is good.

Fig. 4*b* shows the bonded two-layer chips (chip *a*, *b*, *c*) with microchannels, microvalves and other microstructures. Fig. 4*c* shows the bonded five-layer chip (chip *d*). Chip *a* and chip *b* can be used in capillary electrophoresis (CE) analysis. Chip *c* and chip *d* can be used in POCT.

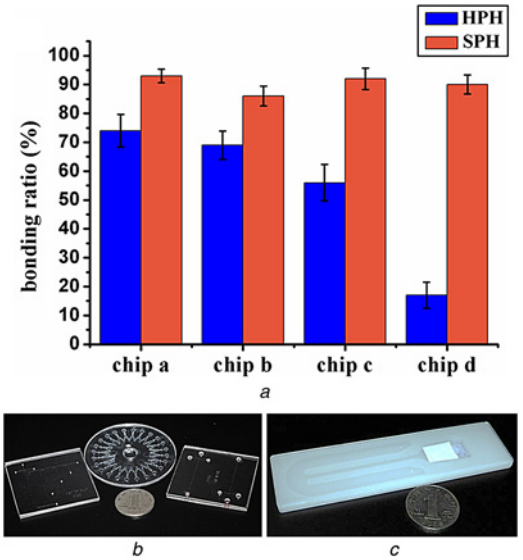

Fig. 4 *SPH results compared with HPH and complete chip images*
a Bonding ratio results between SPH and HPH. The error bar represents the standard deviation based on five independent experiments
b Two-layer chip for CE detection and POCT
c Five-layer chip for point-of-care testing

3.2. Bonding parameters: To remove the air bubbles, the adhesive bonding parameters need to be optimised. Bonding pressure and bonding time are the most important parameters. Firstly, we choose chip a as our subject, and then choose seven levels of 0.08, 0.1, 0.14, 0.16, 0.18, 0.2, and 0.3 MPa to do the single factor experiments. The bonding time is all retained at 5 s. Each experiment is repeated three times. After bonding, the bonding ratios are calculated by using the method mentioned in Section 2.4. Fig. 5*a* shows the relationship between bonding pressure and bonding ratio. Results have shown that with the increase in bonding pressure, the bonding ratio increases pronouncedly. As the pressure increases above 0.2 MPa, the bonding ratio rises above 95%. Its increase becomes slight.

For bonding time, we choose seven levels of 2, 5, 8, 10, 15, 20, and 25 s to perform experiments. The bonding pressures are all chosen as 0.2 MPa. Each level is done three times. Fig. 5*b* shows the relationship between bonding ratio and bonding time. The results show that the bonding ratio will rise with the increase in bonding time. However, as bonding time reaches 25 s, the bonding ratio reaches above 97%. As the bonding time further increases above 25 s, the bonding ratio rises slightly. Considering the time-consuming, the bonding quality and the energy saving, we choose 0.2 MPa and 25 s as the optimum bonding parameters in this Letter.

The adhesive bonding process also can be performed under a heating condition. In some cases, to heat the substrate to a certain temperature may accelerate the removing of the air bubbles. Except for the heating process, to bond a chip within a vacuum condition can also benefit the bonding. However, the processes of heating, cooling, and vacuuming are all time-consuming. They may reduce the bonding efficiency during mass-production. Hence, we perform all the experiments at room temperature in this Letter. The whole bonding process will only cost about 1 min.

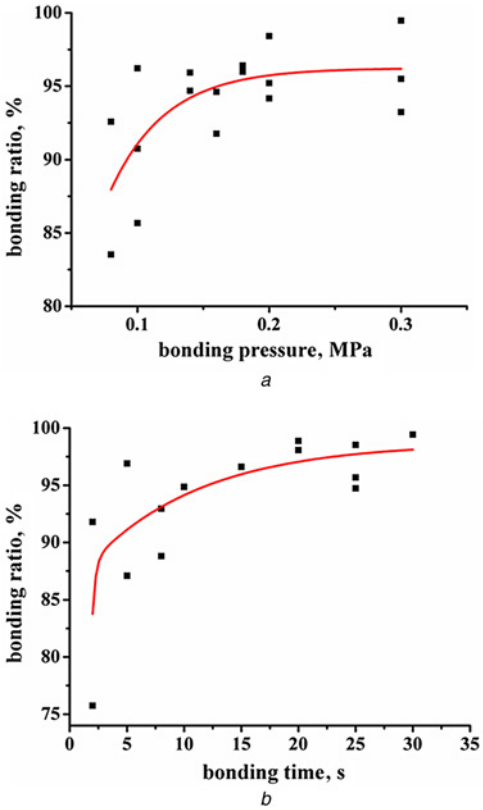

Fig. 5 *Influence of adhesive bonding parameters on bonding ratio*
a Relationship between bonding pressure and bonding ratio
b Relationship between bonding time and bonding ratio

doi: 10.1049/mnl.2016.0478

3.3. Channel residual depth: Channel residual depth is the actual depth as the chip is applied. It may be affected by the deformation of the adhesive film. We found that the deformation mainly relates to the adhesive film thickness and the channel width. The thicknesses of adhesive tape used in the experiments are 25, 50 and 100 µm respectively. Several special chips with different channel widths are fabricated for the experiments. Their channel widths are 150, 200, 500, 1000, 1500 and 2000 µm respectively. Their channel depths are all 100 µm. The method used to measure the channel residual depth has been mentioned in Section 2.4. The results are shown in Fig. 6*a*. As the channel width is below 200 µm, the deformed protrusion of the adhesive film within the channel is only about 5–10 µm, the residual depth of the channel is nearly 90–95 µm. As the channel width increases from 200 to 1000 µm, the decrease in channel residual depth is slight from 5–10 µm to about 10–20 µm. As the channel width increases above 1000 µm, the channel residual depths for 100 and the 50 µm adhesive films both exhibit a sharp decrease from 78–85 µm to nearly 65–72 µm. The channel residual depth for 25 µm adhesive film also exhibits an obvious increase after the channel width above 1000 µm. But it is not sharp as compared with those of the other two conditions. The results show that the channel width has significant effect on the channel residual depth. The reason for this result is that, as the channel increases, the side wall of the channel cannot support the large area of adhesive film. Hence, the centre part of the adhesive film protrudes into the channel.

The experiment profiles in Fig. 6*a* also show the relationship between the adhesive film thickness and the channel residual depth. As the film thickness is 25 µm, the channel residual width changes slightly as the channel width increases. For a channel with a width less than 200 µm, the 25 µm film can ensure the protrusion height of the film into the channel being controlled at about 5–7 µm. As the channel width increases to 1000 µm, the protrusion height of 25 µm film is only about 50% that of 100 µm film, and 67% that of 50 µm film. Then, to seal the chip with 25 µm film will make the channel residual depth being close to the initial channel depth. We think this phenomenon can be explained as follows. As the thickness increases, there are more adhesives can be extruded to flow into the channel. It makes the protrusion height increase and reduce the channel residual depth. Hence, using thin adhesive film to bond a chip can effectively avoid the clogging of the microchannel by adhesives and increase channel residual depth.

Fig. 6*b* shows the SEM images of the cross-sections of the four chips. It can be seen that the deformed protrusion of the film within the channel can be controlled at a small value by using 25 µm film.

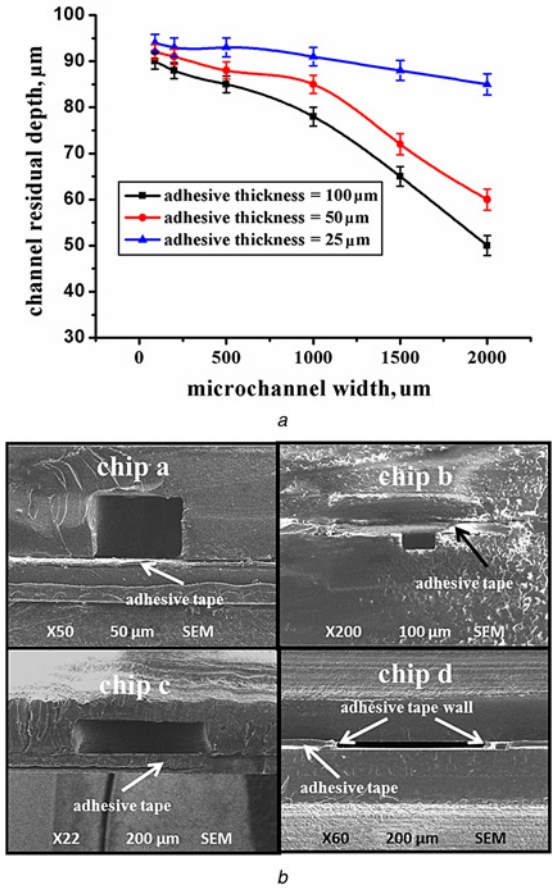

Fig. 6 *Results of channel residual depth*
a Influence of adhesive thickness and microchannel width on channel residual depth. The error bar represents the standard deviation based on five independent experiments
b SEM images of the cross-sections of the four chips

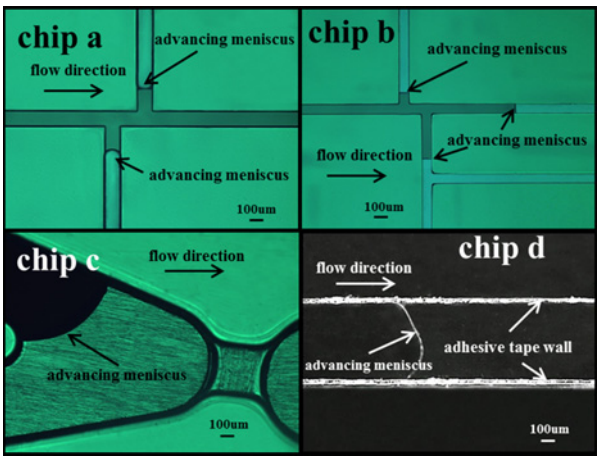

Fig. 7 *Capillary filling process in the channel of all four kinds of microfluidic chips*

3.4. Bonding strength: We use liquid injection test and bonding strength test to measure the bonding strength of the four types of microfluidic devices bonded in this research.

We inject red biological dyes (C0154, Ekear, China) (mixing with DI water) into the microchannels of the four types of microfluidic chips. The microchannels of chip are self-filled at a rate of 64 μms^{-1}. The leakage of liquid from the channel edges is not observed during fluid flow. The experiment is repeated as the capillary filling rate increases to 143 μms^{-1} (we use UV modification to enhance the surface wettability of the channel and enhance the filling rate). No leakage is observed. The results indicate that the adjacent layers in the chip have been sealed completely. Fig. 7 shows the capillary filling process in the channels of all four kinds of microfluidic chips.

The bonding strength is measured by injecting DI water into the channel of a chip with the other end of the channel being closed. A syringe pump (Longer, China) is used as the injecting apparatus. The initial flow rate of the pump is 50 µl/min. As the flow rate reaches 5 ml/min, the DI water begins to leak outside the channel. Basing on the Bernoulli ($Q = \mu A(2P/\rho)^{0.5}$, where Q is flow rate, μ is flow coefficient according to the shape of a channel, A is the area of the channel, P is the pressure difference before and after the channel, ρ is fluid density), bonding strength, which is equal to the leakage pressure, can be derived. The bonding strength of the chip is about 0.504 MPa which can meet the requirement of most kind of microfluidic applications.

4. Conclusions: Our results show that the SHP method can effectively remove the air bubbles from the bonding interface. As

compared with traditional hard head pressing, SHP can obviously enhance the bonding ratio of a microfluidic device, especially in multilayer bonding. By using SHP, the bonding ratio of a microfluidic chip can reach above 95%. The bonding pressure and bonding time are both significant in improving bonding ratio. Our experiments show that the optimal bonding pressure and bonding time for a microfluidic chip are 0.2 MPa and 25 s. The automatic machine developed here can ensure the whole process of chip bonding can be completed within 1 min. The relationship between the adhesive film thickness, channel width and channel residual depth is established. Results show that the channel residual depth will increase as the film thickness reduces. The deformation protrusion of the adhesive film within the channel will decrease as the channel width reduces, which results in the increase in channel residual depth. In this Letter, we choose 25 μm adhesive film to seal the chips. The loss in the depth of the initial channel can be controlled at 5–7 μm for the four types of chips used in this Letter. We use fluid injecting method to measure the bonding strength of the chips. It has been found that the bonding strength can reach 0.504 MPa which can meet the requirements of most microfluidic or POCT applications.

5. Acknowledgment: This work was supported by the National Natural Science Foundation of China (grant nos. 51375076 and 51475079), Science Fund for Creative Research Groups of NSFC (grant no. 51321004) and the National Key Technology R&D Program (2015BAI03B08). This work was also supported by Fundamental Research Funds for the Central Universities (grant no. DUT15LAB12).

6 References

[1] Manz A., Graber N., Widmer H.M.: 'Miniaturized total chemical analysis: a novel concept for chemical sensing', *Sens. Actuators B, Chem.*, 1990, **1**, pp. 244–248

[2] Ren W., Kim H., Lee H.J., *ET AL.*: 'A pressure-tolerant polymer microfluidic device fabricated by the simultaneous solidification-bonding method and flash chemistry application', *Lab Chip*, 2014, **14**, pp. 4263–4269

[3] Satoh A.: 'Water glass bonding', *Sens. Actuators A, Phys.*, 1999, **72**, pp. 160–168

[4] Li J., Chen D., Chen G., *ET AL.*: 'Low-temperature thermal bonding of PMMA microfluidic chips', *Anal. Lett.*, 2005, **38**, pp. 1127–1136

[5] Kistrup K., Poulsen C.E., Hansen M.F., *ET AL.*: 'Ultrasonic welding for fast bonding of self-aligned structures in lab-on-a-chip systems', *Lab Chip*, 2015, **15**, pp. 1998–2001

[6] Thompson C.S., Abate A.R.: 'Adhesive-based bonding technique for PDMS microfluidic devices', *Lab Chip*, 2013, **13**, pp. 632–635

[7] Lago C.L., Silva H.D.T., Neves C.A., *ET AL.*: 'A dry process for production of microfluidic devices based on the lamination of laser-printed polyester films', *Anal. Chem.*, 2003, **75**, pp. 3853–3858

[8] Jena R.K., Chester S.A., Srivastava V., *ET AL.*: 'Large-strain thermo-mechanical behavior of cyclic olefin copolymers: application to hot embossing and thermal bonding for the fabrication of microfluidic devices', *Sens. Actuators B, Chem.*, 2011, **155**, pp. 93–105

[9] Lei K.F., Ahsan S., Budraa N., *ET AL.*: 'Microwave bonding of polymer-based substrates for potential encapsulated micro/nanofluidic device fabrication', *Sens. Actuators A, Phys.*, 2004, **114**, pp. 340–346

[10] Lin C.H., Chao C.H., Lan C.W., *ET AL.*: 'Low azeotropic solvent for bonding of PMMA microfluidic devices', *Sens. Actuators B, Chem.*, 2007, **121**, pp. 698–705

[11] Yu H., Tor S.B., Loh N.H., *ET AL.*: 'Rapid bonding enhancement by auxiliary ultrasonic actuation for the fabrication of cyclic olefin copolymer (COC) microfluidic devices', *J. Micromech. Microeng.*, 2014, **24**, p. 115020

[12] Luo Y., Zhang Z., Wang X., *ET AL.*: 'Ultrasonic bonding for thermoplastic microfluidic devices without energy director', *Microelectron. Eng.*, 2010, **87**, pp. 2429–2436

[13] Im S.G., Bong K.W., Lee C.H., *ET AL.*: 'A conformal nano-adhesive via initiated chemical vapor deposition for microfluidic devices', *Lab Chip*, 2009, **9**, pp. 411–416

[14] Salvo P., Verplancke R., Bossuyt F., *ET AL.*: 'Adhesive bonding by SU-8 transfer for assembling microfluidic devices', *Microfluid. Nanofluid.*, 2012, **13**, pp. 987–991

[15] Lutz R., Oliver S., Bernd F., *ET AL.*: 'Adhesive bonding of microfluidic chips: influence of process parameters', *J. Micromech. Microeng.*, 2010, **20**, p. 087003

[16] Farizah S., Fredrik F., Yitong L., *ET AL.*: 'Dry adhesive bonding of nanoporous inorganic membranes to microfluidic devices using the OSTE(+) dual-cure polymer', *J. Micromech. Microeng.*, 2013, **23**, p. 025021

[17] Goh S.C., Tan S.C., May K.T., *ET AL.*: 'Adhesive bonding of polymeric microfluidic devices'. IEEE Conf. Series: 11th Electronics Packaging Technology Conf., Shangri La, Singapore, December 2009, pp. 737–740

[18] Tan H.Y., Loke W.K., Nguyen N.T.: 'A reliable method for bonding polydimethylsiloxane (PDMS) to polymethylmethacrylate (PMMA) and its application in micro-pumps', *Sens. Actuators B, Chem.*, 2010, **151**, pp. 133–139

[19] Tsao C.W., DeVoe D.L.: 'Bonding of thermoplastic polymer microfluidics', *Microfluid. Nanofluid.*, 2009, **6**, pp. 1–16

[20] Kim J., Shin Y., Song S., *ET AL.*: 'Rapid prototyping of multifunctional microfluidic cartridges for electrochemical biosensing platforms', *Sens. Actuators B, Chem.*, 2014, **202**, pp. 60–66

doi: 10.1049/mnl.2016.0478